Transport of Phosphorus in a Sewage Plume

by

Arnaud L. Morange

Ingénieur, Ecole Centrale Paris
France, 1997

Submitted to the Department of Civil and Environmental Engineering in Partial
Fulfillment of the Requirement for the Degree of

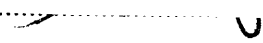Master of Engineering in Civil and Environmental Engineering

at the

Massachusetts Institute of Technology
May 1997

Copyright © 1997 Arnaud L. Morange
All Rights Reserved

The author hereby grants MIT permission to reproduce and to distribute publicly paper
and electronics copies of this thesis document in whole and in part

Signature of Author...

Arnaud L. Morange
May 9, 1997

Certified by...

Bettina Voelker
Assistant Professor
Thesis Supervisor

Accepted by...

Joseph M. Sussman
Chairman, Departmental Committee on Graduate Studies

Transport of Phosphorus in a Sewage Plume

by

Arnaud L. Morange

Submitted to the Department of Civil and Environmental Engineering on May 9, 1997 in Partial Fulfillment of the Requirement for the Degree of Master of Engineering in Civil and Environmental Engineering

Abstract

The Sewage Treatment Plume emanating from the Massachusetts Military Reservation (MMR) located in Cape Cod, Massachusetts, has been contaminated by phosphorus from detergents since 1936. The current phosphorus plume extends 2,500 ft to the south of the source area and intersects Ashumet Pond, thus being of concern to the possible eutrophication of the pond.

In the present study, the mechanisms of transport of phosphorus in this plume are studied. The data were obtained from former studies on the phosphorus plume at MMR by the US Geological Survey (USGS). Two chemical models, an equilibrium model (MINEQL+) and a kinetic model (AcuChem), are applied to the data sets to try to model the sorption behavior of phosphorus in the plume.

It is shown that the equilibrium model provides a reasonable approximation of phosphate sorption behavior on short time scales, although it is unable to predict the observed buffering of pH by the sediments. The kinetic model does not provide significant additional information. It is inconclusive regarding the long-term sorption and desorption behavior of phosphate, since it is based on experiments lasting only a few days. In light of the modeling results, previously published discharge predictions of phosphorus into Ashumet Pond are reexamined and may be underestimated.

Thesis Supervisor: Bettina Voelker
Title: Assistant Professor

Acknowledgments

This thesis stemmed from a group project completed as part of the Master of Engineering program in the Department of Civil and Environmental Engineering. It would not have been possible without the help and dedication of the other members of the group, Julia Choi, Hilary Eichler, Darwin Salipsip, Seth Schneider. Their hard work and assistance is greatly appreciated.

I would like to thank Dr. Pete Shanahan and Bruce Jacobs for their many comments and great help on the group project.

I would also like to thank my advisor, Bettina Voelker, for the incredible number of ideas and reflections she had about the research, and for all the time she spent in making editorial comments and reviewing this thesis. This thesis would never have been written without her help.

Last, I have to thank David H. Marks, Shawn P. Morrissey and Charles H. Helliwell for making this program work the way it does.

TABLE OF CONTENTS

LIST OF UNITS AND ABBREVIATIONS

<u>UNITS</u>

°C - degrees Centigrade

°F - degrees Fahrenheit

$\mu g/L$ - micrograms (10^{-6} grams) per liter

$\mu mol/g$ - micromoles per gram

$\mu mol/L$ - micromoles per liter

ft - feet

g- grams

g/m^3 - grams per cubic meter

hr- hours

$kg\ ha^{-1}\ yr^{-1}$ - kilograms per hectare per year

kg- kilograms

kg/year - kilograms (10^3 grams) per year

L/day- liter per day

m- meter

M- moles per liter

m/day - meters per day

$m^3/year$ - cubic meters per year

mg/L- milligrams (10^{-3} grams) per liter

mg/m^3 - milligrams (10^{-3} grams) per cubic meter

mL- milliliters

mol/L- moles per liter

ABBREVIATIONS

MMR- Massachusetts Military Reservation

STP- sewage treatment plant

USEPA- U.S. Environmental Protection Agency

USGS- United States Geological Survey

TERMS USED IN EQUATIONS

[*Species*]- concentration of the *species*

[*Species*]$_{initial}$- initial concentration of the *species*

k'_1- rate constant for reaction 21

k'_{-1}- rate constant for reaction 22

k'_2- rate constant for reaction 23

K_1- equilibrium constant for reaction 3

k_1- rate constant for reaction 18

k_{-1}- rate constant for reaction 19

K_2- equilibrium constant for reaction 4

k_2- rate constant for reaction 20

K_3- equilibrium constant for reaction 5
Ka_1- equilibrium constant for acid-base reaction 1
Ka_2- equilibrium constant for acid-base reaction 2
ln- the natural logarithm
Log- the base-10 logarithm

CHEMICAL SPECIES

$\equiv$FeOH - sorption site
$\equiv$SH$_2$PO$_4^0$ - neutral sorbed phosphorus
$\equiv$SHPO$_4^-$ - negatively charged sorbed phosphorus
$\equiv$SO$^-$ - negatively charged sorption site
$\equiv$SOH - neutral sorption site
$\equiv$SOH$_2^+$ - positively charged sorption site
$\equiv$SPO$_4^{2-}$ - positively charged sorbed phosphorus
FeP$_1$- sorbed phosphorus
FeP$_2$- diffused sorbed phosphorus
H$^+$ - hydrogen ion
H$_2$O - water molecule
PO$_4^{3-}$ - phosphate

LIST OF FIGURES

LIST OF TABLES

**Figure 1. Concentration of Phosphorus in Groundwater, 1978-1979
(Adapted from LeBlanc, 1984)**

1. INTRODUCTION

1.1 Site background and Problem Statement

Since 1936, treated sewage has been discharged onto 12 acres of rapid infiltration sand beds at the Massachusetts Military Reservation (MMR), in Cape Cod, Massachusetts. This disposal of treated sewage on the site has created a plume of sewage contaminated groundwater, known as the Ashumet Valley sewage plume, in the underlying sand and gravel aquifer.

This study focuses on the transport of phosphorus in the Ashumet Valley plume, which is located upgradient from Ashumet Pond. Phosphates, used in commercial detergents, were present in the treated effluent from the STP, which was discharged to the infiltration beds.

Phosphorus concentrations are high in the part of the STP plume immediately downgradient of the sewage disposal beds. Phosphorus transport in groundwater is retarded by the tendency of phosphorus to sorb onto sediment surfaces, particularly the surfaces of iron oxyhydroxides. Additionally, phosphorus can co-precipitate with metal oxides, further retarding transport. Despite these retardation mechanisms, phosphorus can still be transported in groundwater for considerable distances. In fact, LeBlanc (1984) found that the leading edge of phosphorus contaminated groundwater, as defined by concentrations greater than 0.05 mg/L (50 µg/L), has advanced about 2500 ft downgradient of the sewage disposal beds (Figure 1).

Phosphorus contaminated groundwater discharges into Ashumet Pond. There is concern that discharge of phosphorus into the pond, which is currently considered mesotrophic, will increase nutrient concentrations and cause the pond to become eutrophic. Sewage disposal was stopped on the military reservation in December 1995. The fate of phosphorus sorbed to aquifer sediments following the introduction of uncontaminated groundwater into the aquifer is of particular concern to the local community; the possible desorption and remobilization of sorbed phosphorus may adversely affect the ecology of Ashumet Pond for many years.

The purpose of the study is to evaluate the geochemical processes that affect the mobility of phosphorus in the sand and gravel aquifer, and to determine how phosphorus mobility may change after sewage disposal ceases.

1.2 Hydrogeologic Setting

Ashumet Valley is located on what is known as Inner Cape Cod. The Inner Cape consists of moraines formed by the melting and advancing of glaciers. These moraines are predominantly composed of till. Subsequent advancing and retreating of glaciers around the Cape led to the development of kettle hole ponds by ice that remained and later melted. Ashumet Pond is one such kettle hole pond. Soil profiles in the pond watershed show sandy topsoils with sandy loam to gravelly sand underlain by sand or gravel. Beneath the topsoil lies approximately 150 feet of generally well sorted, light brown, medium to very coarse sand with some presence of gravel. Below this layer exists approximately 100 ft of very fine sand with some silt. These unconsolidated deposits, which are highly permeable, sit on a crystalline bedrock made predominantly of granodiorite. The bedrock elevation dips in a southeast direction towards Ashumet Pond. Analysis of an aquifer test conducted in sand and gravel deposits by the USGS, about 1000 ft downgradient of the sewage disposal beds, yielded an average hydraulic conductivity of 380 ft/d and a porosity of 0.39.

The ground water flow system of western Cape Cod is unconfined. Groundwater flows radially outward from a water table mound located to the north of the study area. This water table mound has a maximum hydraulic head of about 70 ft above sea level. In the study area, groundwater flow is southward and water table elevations range from 44 to 49 ft above sea level. During periods of increasing pond stage, hydraulic gradients in the area between the infiltration beds and the pond increase and groundwater flow directions shift eastward toward the pond. Groundwater flow up-gradient from the pond is predominantly horizontal. Vertical gradients near the pond shore are significantly higher because of the strong local effect of the pond. Precipitation is the sole source of

natural recharge to the aquifer, and groundwater discharges to streams and coastal embayments. Groundwater flow occurs primarily within the coarse grained sediments. The saturated thickness of these sediments is about 120 ft in the study area.

2. METHODOLOGY AND RESULTS

2.1 Goals and Objectives

The goal of this study is to use chemical models to find explanations for the results of experimental studies done by the USGS, and to link these results to field observations. The data used are available in two USGS reports on phosphorus transport by Donald Walter and co-workers (1995, 1996). These reports contain the physical data for well-cluster sites used to collect water quality samples and water level measurements near Ashumet Pond. These reports also contain: (1) phosphorus profiles versus depth at different wells (2) concentration profiles at different depths (3) results from batch sorption experiments (4) column experiments and (5) different results from the modeling done by the USGS.

The main focus is thus to reexamine the data with two chemical models, a kinetic model and an equilibrium model. These two models are calibrated with the results of the batch experiments. The models are then used to determine which part of the column experiments can be explained with kinetic and equilibrium batch studies, what other explanations are needed, and implications for the transport of phosphorus in groundwater. The results are used to estimate future discharge of phosphorus into Ashumet Pond as clean water flows through the aquifer.

2.2 Description of the available data

The experimental and field data described below are provided by the different experiments performed by the USGS at the site (Walter et al., 1995; Stollenwerk, 1995; Stollenwerk 1996).

2.2.1 Batch experiments

The first experiment was conducted to determine the rate of phosphorus sorption onto uncontaminated sediments. Sixteen samples were prepared for two initial phosphorus concentrations (31 mg/L and 3.1 mg/L) with 15 g of dry uncontaminated sediment and 25 mL of artificial groundwater. The concentration of phosphorus in the solution of the samples was measured at different times (4 to 240 hours). Figure 2 shows adsorption curves according to the data by Walter et al. (1995).
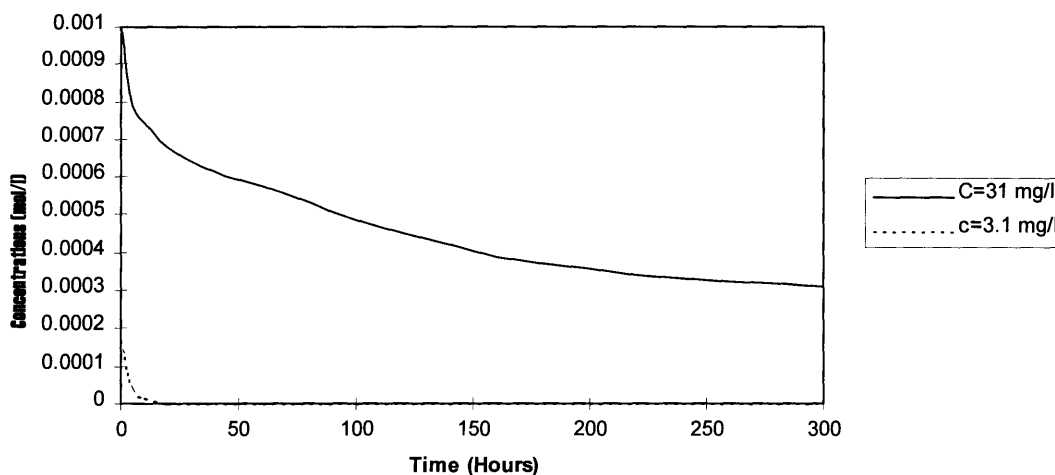
Figure 2. Experimental Adsorption

A second experiment was conducted to determine adsorption isotherms of phosphorus on uncontaminated and contaminated sediments. Using solutions of artificial groundwater with concentrations of phosphorus ranging from 0.15 to 31 mg/L, samples were prepared using 15 g of sediment and 25 mL of water, with pH adjusted to 6.0. The concentrations of phosphorus in the solutions were measured after equilibrating 48 hours.

12

Figure 3 shows adsorption isotherms according to the data by Walter et al. (1995).
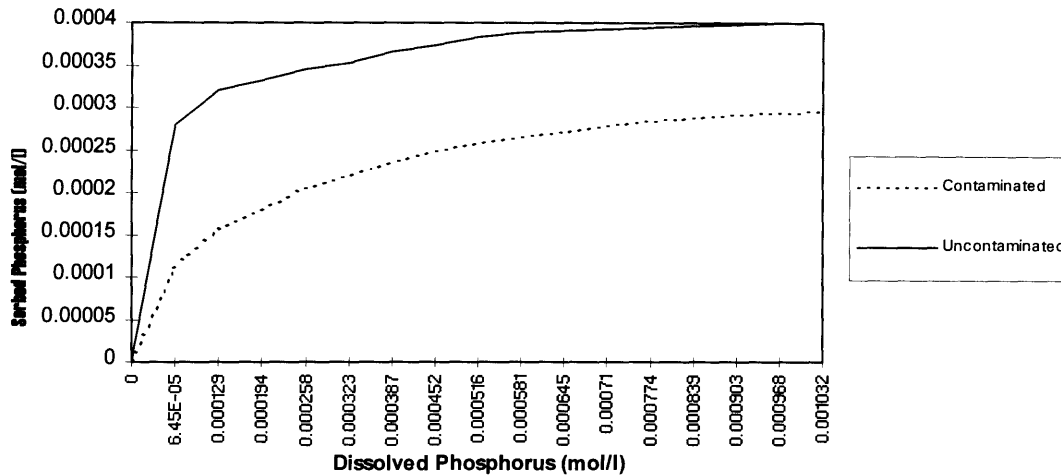
Figure 3. Experimental Isotherms

A batch desorption experiment was conducted to determine the rate of phosphorus desorption under conditions similar to those found in the uncontaminated part of the aquifer. Samples were prepared using sediments from eight subsections obtained from beneath the disposal beds mixed with artificial uncontaminated groundwater. Fifteen grams of sediment and 25 mL of water were mixed and the pH was measured. Solutions were removed from the samples at specific time intervals, and the concentration of phosphorus was measured; uncontaminated artificial groundwater was then added back to the sample. The results are shown on Figure 4 for two of the subsections.
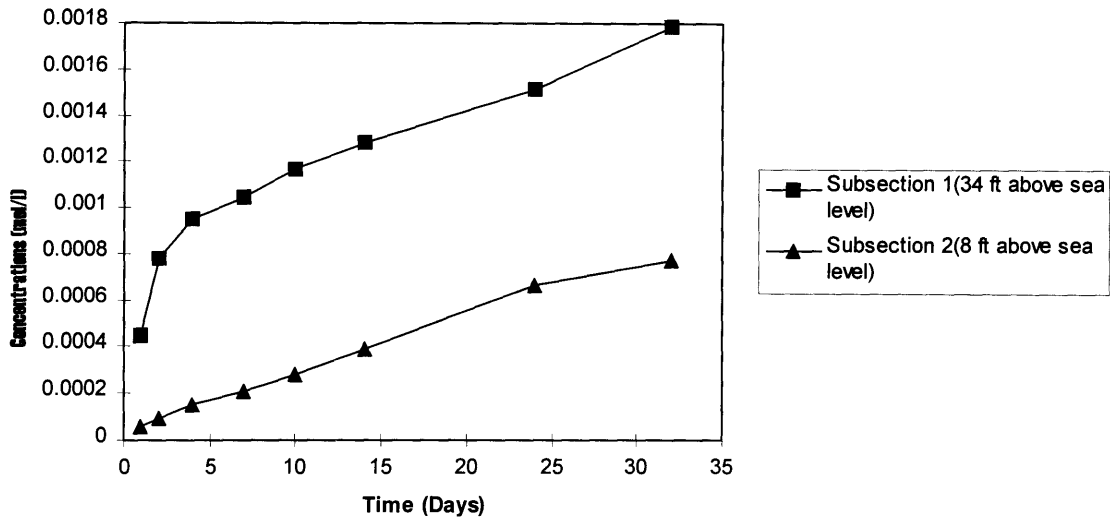
Figure 4. Experimental Desorption

Adsorption isotherms as a function of pH were determined for phosphate (PO_4^{3-}) using artificial groundwater and uncontaminated sediments. The results are plotted in terms of percent solute adsorbed as a function of pH. These isotherms were determined for two initial concentrations of phosphorus C_1 and C_2 (where C_1=600 μmol/l and C_2=105 μmol/l). The results of this experiment are shown on Figure 5.
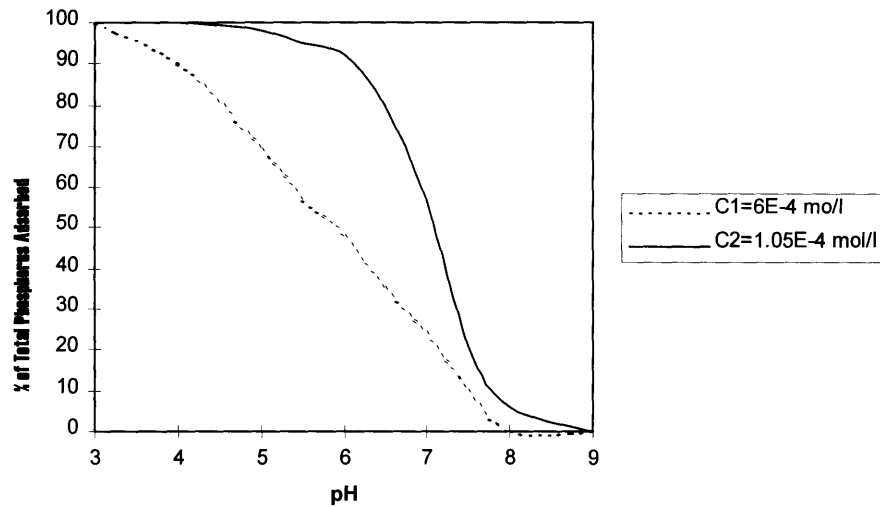
Figure 5. pH Isotherms

2.2.2 Column Experiments

Column experiments were conducted on uncontaminated and contaminated samples to determine the extent of phosphorus sorption and desorption in conditions simulating the aquifer. A flow of contaminated groundwater was flushed through four columns containing uncontaminated sediments from the unsaturated zone. Phosphorus concentrations in two of the columns were C_3=0.49 mg/L. In the two other columns, the concentration was increased to C_4=6.1 mg/L. In all columns, sewage contaminated groundwater was flushed through the columns until the concentrations in the effluent approached influent concentrations and stabilized. Uncontaminated groundwater was then flushed through the columns. Figures 6a and 6b reproduce the data by Walter et al. (1995).

Figure 6. Column Experiments
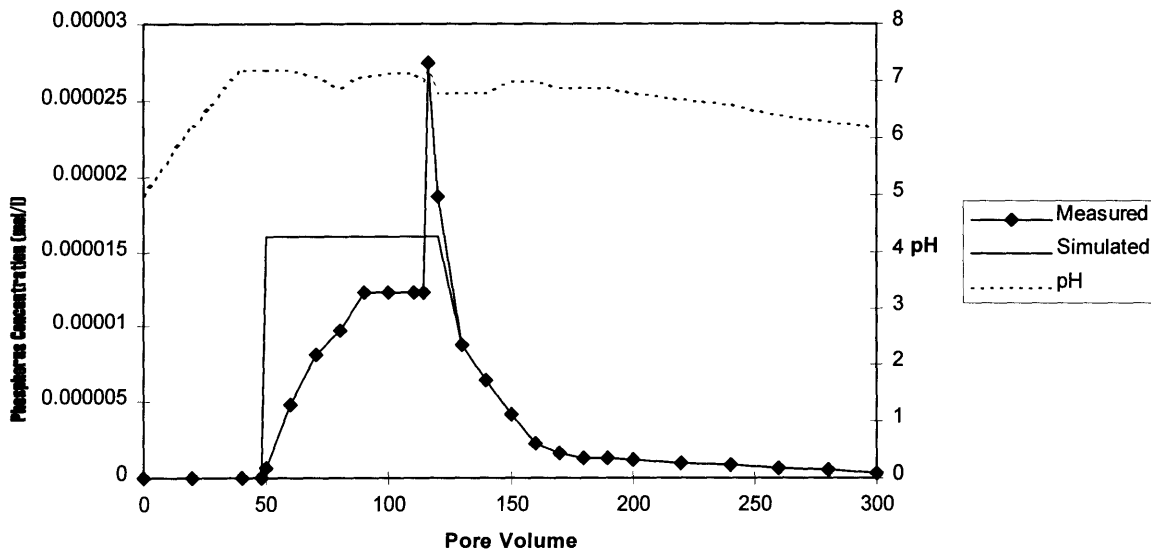
Figure 6a. Column Experiment with C_3=0.49 mg/L=16 μmol/l
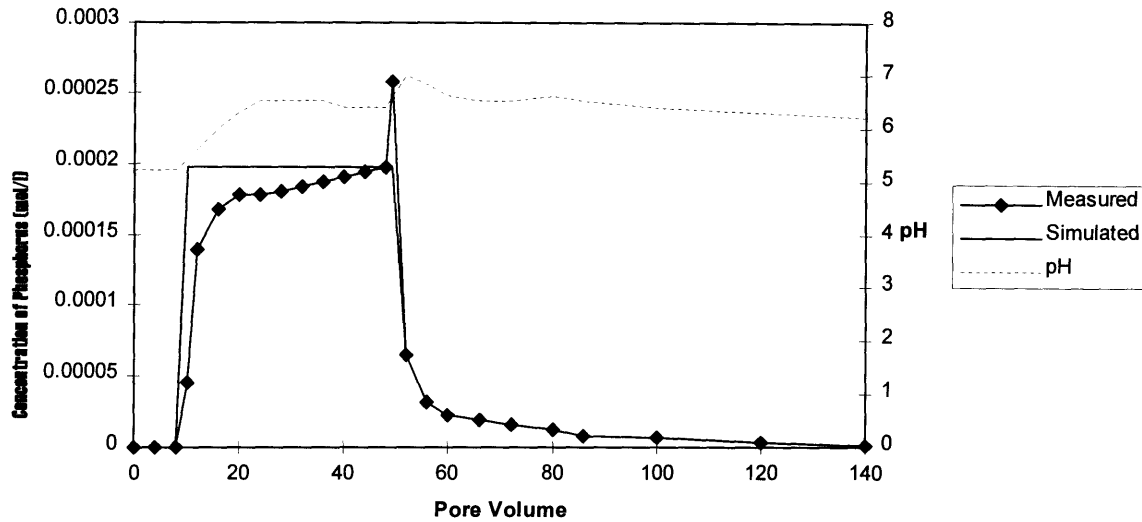
Figure 6b. Column Experiment with C_4=6.1 mg/L=200 μmol/l

2.3 Equilibrium Data Analysis

2.3.1 The Equilibrium Model

The goal of the first part of the research on phosphorus sorption was to obtain a computer model to simulate the equilibrium sorption or desorption of phosphorus. The complex chemistry necessitated the use of a surface complexation model to simulate PO_4^{3-} adsorption. Chemical reactions at the solid-solution interface are treated as surface complexation reactions analogous to the formation of complexes in solution. The software chosen to simulate the system is MINEQL+™, a recent adaptation of the original MINEQL (Westall et al., 1976). The adsorption on hydrous ferric oxides using MINEQL+™ can be described by an electric double layer model (Dzombak and Morel, 1990).

The first reactions that are modeled are two acid-base reactions involving the different surface species of hydrous ferric oxides: $\equiv$SOH, $\equiv$SOH$_2^+$, and $\equiv$SO$^-$.

16

These reactions are:

$$\equiv \text{SOH} + \text{H}^+ == \equiv \text{SOH}_2^+ \qquad K_{a_1} = \frac{[\equiv SOH_2^+]}{[H^+] \times [\equiv SOH]} \qquad (1)$$

$$\equiv \text{SOH} = \equiv \text{SO}^- + \text{H}^+ \qquad K_{a_2} = \frac{[H^+] \times [\equiv SO^-]}{[\equiv SOH]} \qquad (2)$$
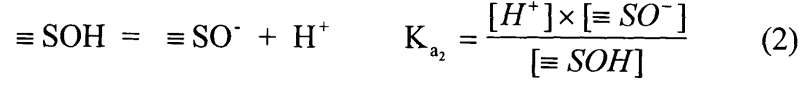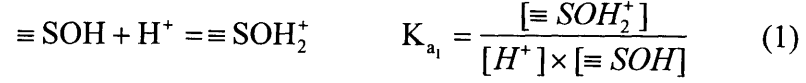
The equilibrium constants K_{a1} and K_{a2} are the first two adjustable parameters of the system.

Next, the adsorption of phosphorus on the oxides is modeled. These processes are described by the following reactions:

$$\equiv \text{SOH} + \text{PO}_4^{3-} + 3\text{H}^+ == \equiv \text{SH}_2\text{PO}_4^0 + \text{H}_2\text{O} \quad K_1 \qquad (3)$$

$$\equiv \text{SOH} + \text{PO}_4^{3-} + 2\text{H}^+ == \equiv \text{SHPO}_4^- + \text{H}_2\text{O} \quad K_2 \qquad (4)$$

$$\equiv \text{SOH} + \text{PO}_4^{3-} + \text{H}^+ == \equiv \text{SPO}_4^{2-} + \text{H}_2\text{O} \quad K_3 \qquad (5)$$
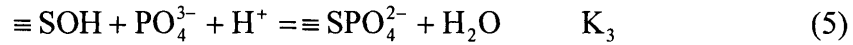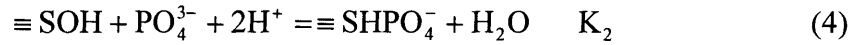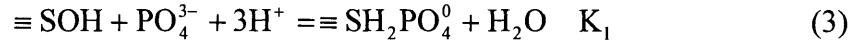
The equilibrium constants K_1, K_2, and K_3 are three other adjustable parameters for the system. The last variable parameter is the total site concentration:

$$[\equiv\text{SOH}]_T = [\equiv\text{SOH}] + [\equiv\text{SOH}_2^+] + [\equiv\text{SO}^-] + [\equiv\text{SH}_2\text{PO}_4^0] + [\equiv\text{SHPO}_4^-] + [\equiv\text{SPO}_4^{2-}] \quad (6)$$

2.3.1.1   Determination of Constants

The calibration of the model (i.e. the determination of variable parameters) was performed using the data described in the previous section. The constants were determined to fit the following batch experiment data: the adsorption isotherms (Figure 3), and the pH isotherms (Figure 5).

There were several options in the calibration process: given the amount of time and data available, it was not possible to adjust all of the six adjustable parameters. Therefore, some of the parameters had to be fixed prior to the calibration.

17

For the constants K_{a_1} and K_{a_2}, Stollenwerk adjusted them to 6.3 and -7.1 respectively. All other parameters being equal, Stollenwerk's constants always provided better results (i.e. a better fit) than those in MINEQL+'s database (i.e. Dzombak and Morel's). Therefore, the chosen acid-base thermodynamic constants are:

$$\text{Log } K_{a_1} = 6.3 \tag{7}$$

$$\text{Log } K_{a_2} = -7.1 \tag{8}$$

For the constants K_1, K_2, and K_3, Stollenwerk adjusted these constants to 27.8, 21.6 and 16.5 respectively (Stollenwerk, 1995). All other parameters being equal, these constants provided the better fit. Therefore, the chosen adsorption thermodynamic constants are:

$$\text{Log } K_1 = 27.8 \tag{9}$$

$$\text{Log } K_2 = 21.6 \tag{10}$$

$$\text{Log } K_3 = 16.5 \tag{11}$$

2.3.1.2 Determination of the number of sites

The number of sites was the main variable parameter. The adsorption site density in most of the models is given in micromoles per gram of sediment (μmol/g). Stollenwerk determined a site density of 1.1 μmol/g using a titration with H^+ (1995).

Another estimate of the surface site concentration is provided by the maximum amount of phosphorus sorbed in the USGS data.

For uncontaminated sediments:

On Figure 3 we read: $[Sorbed\ Phosphorus]_{MAX} = 21\,mg\,/\,kg$

Thus:
$$[Sites] = \frac{[Sorbed\ Phosphorus]_{MAX}}{M_P} = \frac{21\,mg\,/\,kg}{31\,g\,/\,mol} = 0.67\,\mu mol\,/\,g \tag{12}$$

For contaminated sediments:

On Figure 3 we read: $[Sorbed\ Phosphorus]_{MAX} = 15\,mg\,/\,kg$

Thus: $$[Sites] = \frac{[Sorbed\ Phosphorus]_{MAX}}{M_P} = \frac{15\,mg\,/\,kg}{31\,g\,/\,mol} = 0.49\,\mu mol\,/\,g \quad (13)$$

These results are based on the maximum amount of sorbed phosphorus and are only part of the total number of sites. The value chosen in this study for the total number of sites is 0.9 μmol/g, which is a lower value than the value of 1.1 μmol/g used in the USGS study and higher than the values estimated from the pH sorption isotherms, but which provided optimum results in the modeling of the data in Figure 5.

We can use this value to discuss the results from the column experiments (Figure 6a and 6b): on Figure 6a we see a sharp breakthrough occurring after 45 pore volumes. This corresponds to the number of pore volume required until all the sites are in equilibrium with the input concentration of dissolved Phosphorus. We can calculate the number of pore volumes necessary to saturate the maximum number of sites calculated above and compare it to the value given by Figures 6a and 6b.

For the first experiment (Figure 6a):

$$C_3 = 0.49\,mg\,/\,l = \frac{0.49\,mg\,/\,l}{M_p} = 1.6 \times 10^{-5}\,mol\,/\,l \quad (14)$$

Since we have in each column v=154.4 cm^3 of sediment with a porosity n=0.33 and a bulk density d=1.68 g/cm^3, then it follows that:

$$m_{sediments} = v \times d = 259\,g \quad and \quad V_{pore\ volume} = v \times n = 51\,cm^3$$

Therefore,

$$[Sites] = 0.9\,\mu\,mol\,/\,g = 0.9 \times 10^{-6} \times \frac{259}{51 \times 10^{-3}} = 4.57 \times 10^{-3}\,mol\,/\,l\ of\ pore\ volume$$

Thus, the number of pore volumes required to saturate these sites should be:

$$N = \frac{[Sites]}{C_3} = \frac{4.57 \times 10^{-3}}{1.6 \times 10^{-5}} = 285$$

If we compare this with the actual 45 pore volumes, we see that only about 20% of the sites seem to be saturated.

For the second experiment (Figure 6b):

$$C_4 = 6.1\, mg\,/\,l = \frac{6.1\, mg\,/\,l}{M_p} = 1.96 \times 10^{-4}\, mol\,/\,l \qquad (15)$$

and

$$[Sites] = 4.57 \times 10^{-3}\, mol\,/\,l$$

Thus:

$$N = \frac{4.57 \times 10^{-3}}{1.96 \times 10^{-4}} = 23$$

In this last case, about 33% of the sites seem to be saturated.

We can compare these two percentages of saturated sites with the two percentages calculated with MINEQL+, using a pH of 6.3 (the measured pH of the contaminated sediments in the column experiments was 6.2-6.5) and dissolved phosphorus concentrations of C_3=0.49 mg/l and C_4=6.1 mg/l. We have the following results: for C_3=0.49 mg/l, we find that 25% of the sites are saturated; for C_4=6.1 mg/l, we find that about 37% of the sites are saturated. The results are consistent with what was observed in the column experiments. The slightly higher values can be explained by the fact that MINEQL+ does not take kinetics into account.

Both these results show that under these conditions, the adsorption occurs on the lower part of the adsorption isotherm (See Figure 3); the phosphorus does not occupy all available sites.

We can also use the value of total number of sites to compare the concentrations of sites in the batch experiments and in the real system (i.e. the aquifer).

For the batch experiments we have samples made with a mass m_1 of sediments and a volume v_1 of water, thus:

$$[Sites(mol\ /\ l)] = \frac{[Sites(mol\ /\ g)] \times m_1}{v_1} = \frac{0.9 \times 10^{-6} \times 15}{25 \times 10^{-3}} = 5.4 \times 10^{-4}\ mol\ /\ l \quad (16)$$

For the real system, we have a density d, a porosity n: per 1 l sample, we have $n*1l=330$ ml water and $m=d*1000=1680$ g of sediment. Thus:

$$[Sites(mol\ /\ l)] = \frac{[Sites(mol\ /\ g)] \times 1680g}{0.33l} = 4.6 \times 10^{-3}\ mol\ /\ l \quad (17)$$

The value is higher in the real system than in the experiments, by a factor of approximately 10. This difference shows that the batch experiments are not fully representing the system. It can be suggested for new experiments, that the soil to water ratio should be higher, to have a higher concentration of sites.

2.3.2 Results of the MINEQL+™ modeling
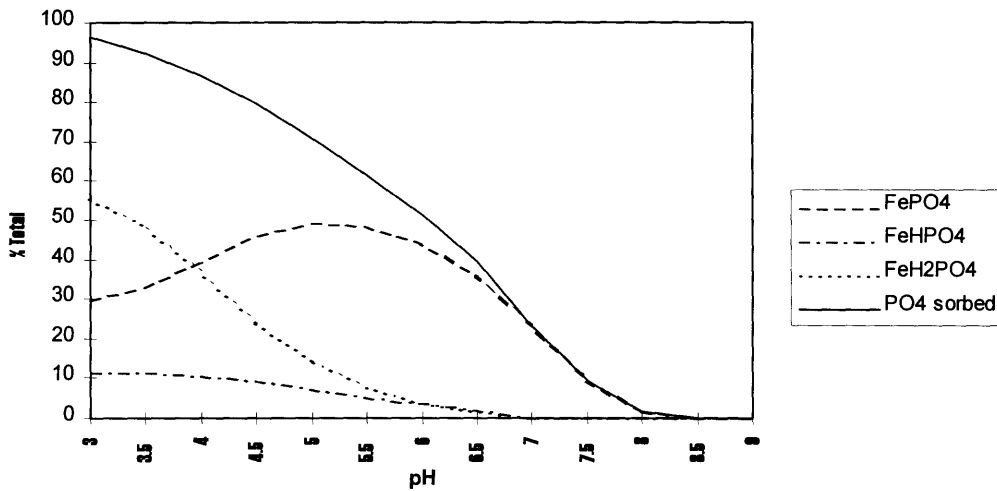
Figure 7. Modeled Isotherm for C_1=600 μmol/l

The first task was to reproduce the data from the two batch experiments for pH isotherms (i.e. the data of Figure 5). Using the constants given above for MINEQL+™, we obtained the results shown in Figures 7. An acceptable data fit (with an error of around 10%) is obtained by superimposing the experimental results and the modeled results as shown in Figure 8a and Figure 8b. MINEQL+™ is thus able to reproduce the adsorption behavior as a function of pH, which is the expected result, since these data were used to calibrate the model. It can be seen from these two pH isotherms that, at the considered range of pH in the groundwater (i.e. 5 to 8), only part of the phosphorus is sorbed. Furthermore, the general trend is toward a decrease of the sorbed phosphorus with an increase in pH.

Figure 8. Comparison of Modeled and Experimental Isotherms
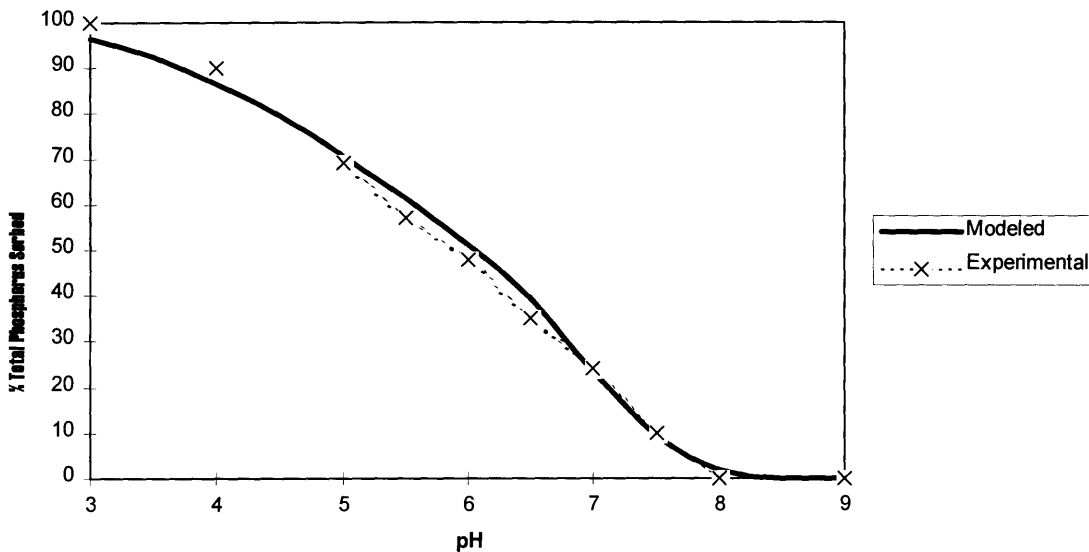
Figure 8a. Comparison of Modeled and Experimental Isotherms for C1=600 μmol/l
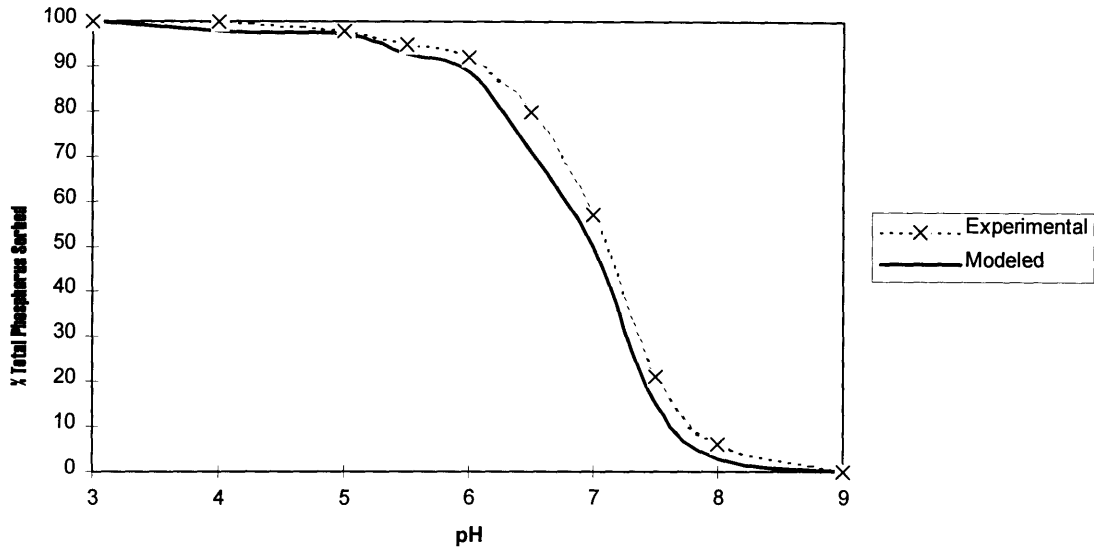
Figure 8b. Comparison of Modeled and Experimental Isotherms for

C_2=105 µmol/l

The second task was to reproduce the adsorption isotherms. There are two different experimental isotherms, one for contaminated and one for uncontaminated groundwater, as shown on Figure 3. The modeled isotherm was obtained from MINEQL+™ by varying the total concentration of phosphorus. The result of the model is the isotherm shown on Figure 9.

By superimposing this isotherm with the experimental isotherms, we see that it fits between both isotherms (see Figure 9). The contaminated isotherm is significantly lower than the uncontaminated isotherm in the experiments because some sites are already occupied in the contaminated sediments. However, MINEQL+™ does not reproduce the steep slope of the isotherms at low phosphorus concentrations. This strong adsorption might be evidence of the existence of a small quantity of strong binding sites, which are not taken into account by MINEQL+™ (only weak sites are considered in the model).
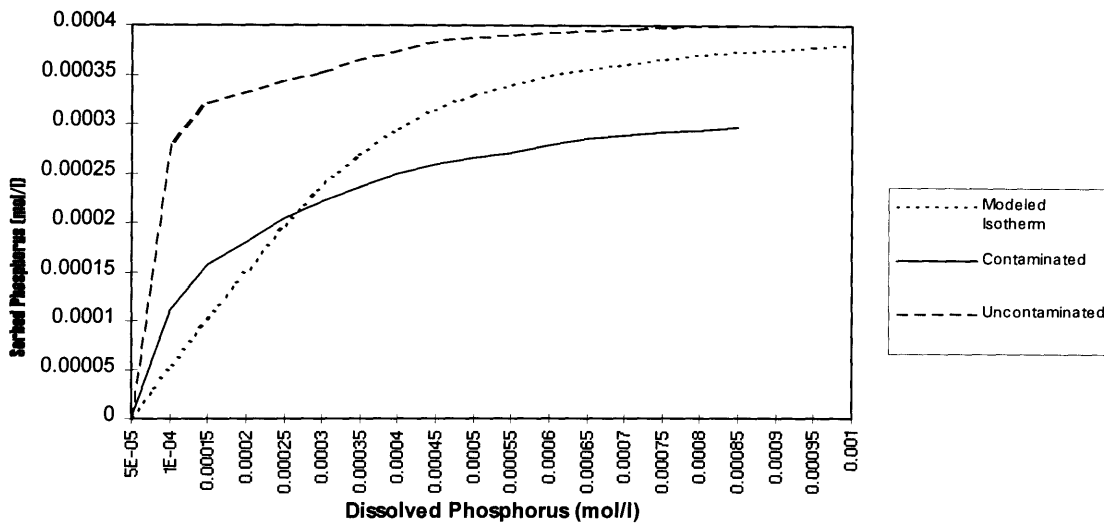
Figure 9. Comparison of Modeled and Experimental Isotherms

2.4 Kinetics Data Analysis

2.4.1 Adsorption Kinetics Model

The results of the batch experiment on adsorption show a two step adsorption process. The first step is a fast adsorption process, lasting approximately 48 hours, followed by a slower process. The software used to simulate this adsorption is AcuChem™ (Braun et al, 1988). This program reads an input file containing the different reactions, their rate constants, and the initial concentrations and solves the resulting system of differential equations numerically.

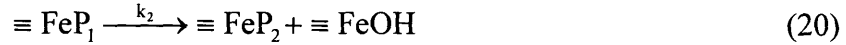Two different conceptual models may be used to explain the two step adsorption process (Goldberg, 1984; Robertson, 1995). The first hypothesis postulates an initial rapid adsorption of phosphorus onto the surface of the metal oxide. Once the phosphorus is sorbed onto the surface, it will diffuse further into the metal oxide via a slower process. This process can be modeled by including the following reactions in the AcuChem input:

Fast Adsorption and Desorption

$$\equiv FeOH + PO_4^{3-} \xrightarrow{\;k_1\;} \equiv FeP_1 \tag{18}$$

$$\equiv FeP_1 \xrightarrow{\;k_{-1}\;} \equiv FeOH + PO_4^{3-} \tag{19}$$

Slow Diffusion

$$\equiv FeP_1 \xrightarrow{\;k_2\;} \equiv FeP_2 + \equiv FeOH \tag{20}$$

where $\equiv FeOH$ represents the sites, $\equiv FeP_1$ represents sorbed phosphorus, and $\equiv FeP_2$ represents diffused sorbed phosphorus.

For simplicity, the speciation of sites and solution species are ignored in this description. Therefore, the rates constants represent apparent (pH dependent) values.

The second hypothesis postulates a rapid adsorption of the phosphorus onto the surface of the metal oxide. This rapid adsorption creates a thin layer of mixed phosphorus and metal oxide. The phosphorus then must diffuse through this thin layer to sorb onto the sediment surface. This diffusion is the second, slower process. This second process can be modeled by the following reactions:

Fast Adsorption and Desorption

$$\equiv FeOH + PO_4^{3-} \xrightarrow{\;k_1'\;} \equiv FeP_1 \tag{21}$$

$$\equiv FeP_1 \xrightarrow{\;k_{-1}'\;} \equiv FeOH + PO_4^{3-} \tag{22}$$

Slow Diffusion

$$PO_4^{3-} \xrightarrow{\;k_2'\;} \equiv FeP_2 \tag{23}$$

The first reaction is the same for the two mechanisms (although the rate constants k_1 and k_{-1} might be different than k_1' and k_{-1}' for the calibration) and is described by second order kinetics. However, the second (slow) reaction is subject to differences in interpretations. The first mechanism (see Equation 20) assumes that the phosphorus that is sorbed will diffuse. Therefore, no other phosphorus molecules are used by the

reaction, and a site is regenerated. The second mechanism (see Equation 23) assumes that another phosphorus molecule diffuses through the layer and that no site is regenerated.

2.4.1.1 Determination of the rate constants

The first step of the calibration of AcuChem™ was to determine the rate constants. The rates k_1 and k_{-1} can be related to the apparent equilibrium constant of the fast adsorption reaction as follows:

$$K_{app} = \frac{k_1}{k_{-1}}, \text{ where } K_{app} = \frac{[Sorbed \quad P]}{[FreeSites] \times [Dissolved \quad P]}.$$

K_{app}, which is pH dependent, can be calculated from the binding constants used in our equilibrium model. The experimental adsorption isotherms are obtained for uncontaminated sediments. Therefore, a pH of 5.5 was chosen, corresponding to the pH in uncontaminated sediments. At that pH, the main adsorbed species is $\equiv SPO_4^{2-}$ and the main other surface species is $\equiv SOH$. The equilibrium we will refer to is given by equation (5), and the value of the constant is $K_3 = 16.5$. We have:

$$K_3 = \frac{[\equiv SPO_4^{2-}]}{[\equiv SOH] \times [PO_4^{3-}] \times [H^+]} = 10^{16.5}$$

Thus, at pH=5.5, we have: $\dfrac{[\equiv SPO_4^{2-}]}{[\equiv SOH] \times [PO_4^{3-}]} = 10^{16.5} \times 10^{-5.5} = 10^{11}$

For the first isotherm, we have [Phosphorus]$_{initial}$=[PO_4^{3-}]$_T$=31 mg/l=1x10^{-3} mol/l. Therefore, if pH=5.5, the speciation for phosphorus according to acid-base chemistry is for PO_4^{3-}: $[PO_4^{3-}]$=2.7x10^{-11} mol/l.

Thus, $\dfrac{[\equiv SPO_4^{2-}]}{[\equiv SOH]} = 10^{11} \times 2.7 \times 10^{-12} = 0.27 \qquad (24)$

But equations (18) and (19) give: $\dfrac{k_1}{k_{-1}} = \dfrac{[\equiv FeP_1]}{[\equiv FeOH] \times [PO_4^{3-}]_T} = \dfrac{[\equiv SPO_4^{2-}]}{[\equiv SOH] \times [PO_4^{3-}]_T}$

Using (24), we have: $\dfrac{[\equiv SPO_4^{2-}]}{[\equiv SOH]} = 0.27$ and since $[PO_4^{3-}]_T = 1 \times 10^{-3} mol / l$, we find:

$$\frac{k_1}{k_{-1}} = 2.7 \times 10^2 \qquad (25)$$

For the second isotherm, we have [Phosphorus]$_{initial}$=3.1 mg/l=1x10^{-4} mol/l. Similar

calculations give the same ratio for $\frac{k_1}{k_{-1}}$.

This ratio is the same for the two mechanisms: $\frac{k_1}{k_{-1}} = \frac{k_1'}{k_{-1}'} = 270$

For the first mechanism, [$\equiv$FeOH]$_{initial}$=[Sites]$_{initial}$=5.4x10^{-4}mol/l (see Equation 10).

Because [Phosphorus]$_{initial}$ is fixed, k_1 and k_2 are the only two adjustable parameters for

AcuChem™. Likewise, k_1' and k_2' are the only two variable parameters for the second

mechanism.

The conditions chosen to represent the first mechanism are as follows:

- [Sites]$_{initial}$=5.4x10^{-4}mol/l
- [PO$_4^{3-}$]$_{initial}$=1x10^{-3}mol/l=31mg/L
- k_1=60 hr^{-1}
- k_{-1}=0.222 hr^{-1}
- k_2=4.0x10^{-2} hr^{-1}

The conditions chosen to represent the second mechanism are as follows:

- [Sites]$_{initial}$ =5.4x10^{-4}mol/l
- [PO$_4^{3-}$]$_{initial}$ =1x10^{-3}mol/l =31mg/L
- k_1' =100 hr^{-1}
- k_{-1}' =0.37 hr^{-1}
- k_2' =6.0x10^{-3} hr^{-1}

2.4.2 Results of the AcuChem™ Modeling

The results of the AcuChem™ modeling to simulate phosphorus adsorption are
shown on Figure 10a for the first mechanism and on Figure 10b for the second
mechanism.

Figure 10. Modeled Adsorption
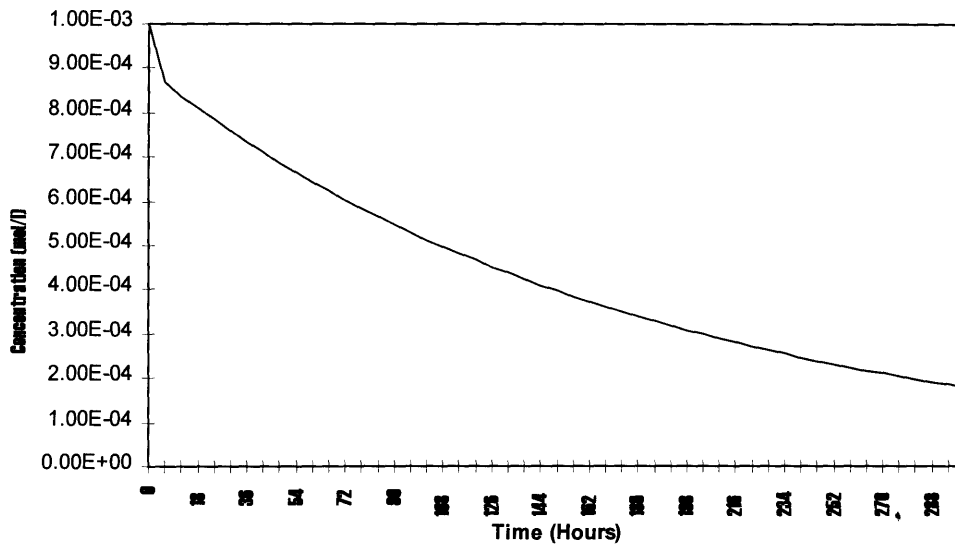
Figure 10a. Modeled Adsorption with Mechanism 1
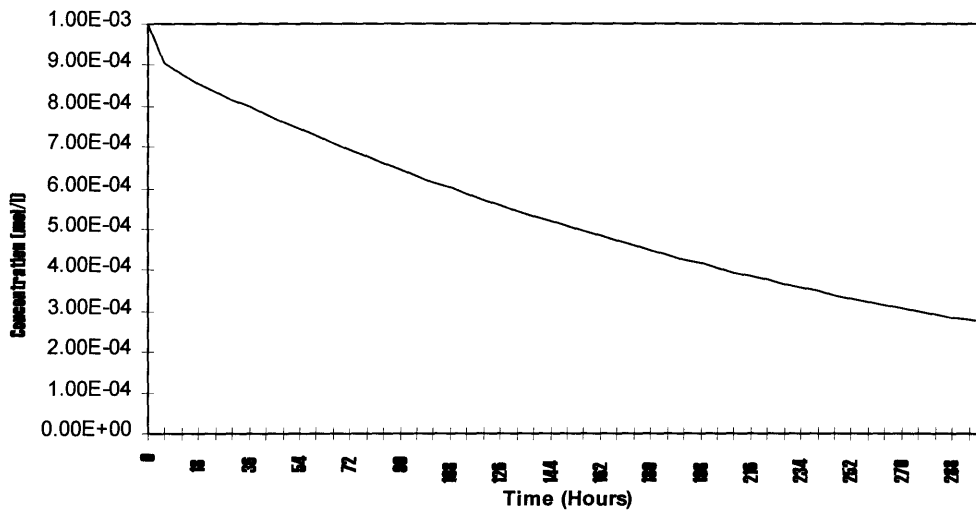
Figure 10b. Modeled Adsorption with Mechanism 2

28

It can be seen that both mechanisms qualitatively fit the experimental adsorption data (Figure 11). Therefore, it is not possible to eliminate one of the hypotheses solely on the basis of AcuChem™ modeling results. The modeling results and the experimental data suggest that the fast adsorption process described in Section 2.4.1 appears to last for more than 48 hours. However, it is not possible to verify the actual active time period for this fast process. Since the equilibration time for the batch experiments, which determined adsorption isotherms, was chosen to be 48 hours, the applicability of such "equilibrium" isotherms is limited. Another limitation of the isotherms stems from the time-scale of the experiments compared to the amount of time that has passed since sewage was first discharged at the site. On a field time-scale, slow processes can take place, and the experiments fail to reproduce these processes which have time scales far greater than 48 hours.
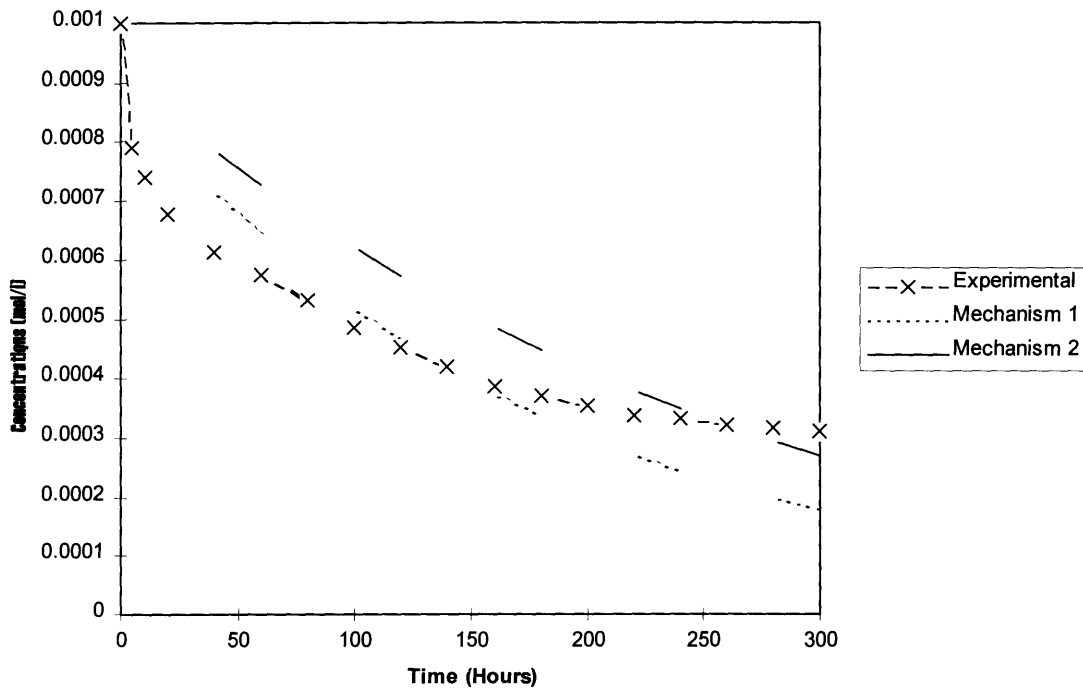
Figure 11. Comparison of Experimental and Modeled Adsorption

2.4.3 Desorption Kinetics Data Analysis

The data on desorption kinetics are not as easy to manipulate as the data on adsorption. The first problem is that the desorption kinetics experiment has been conducted to emulate the conditions of uncontaminated groundwater flushing through the contaminated soil. This emulation required fresh water to be introduced into the samples at specific time intervals. The desorption data shown on Figure 4 shows the cumulative amount of phosphate released with successive introduction of fresh water, and cannot be compared directly to the adsorption isotherms of Figure 3.

It would seem that there is some kinetic information contained in the shape of these curves, which all have the same slope after 4 or 5 days. However, this constant slope, given the experimental conditions, can be interpreted in various ways. The seemingly constant release of phosphate over time can be the result of zero order desorption kinetics (or a process that can be approximated as a zero order). This would indicate that desorption (at least in its second phase) does not correspond to the reverse reactions of the adsorption process. But a constant slope could also be obtained with first order kinetics desorption (corresponding to the reverse reactions of the adsorption process) or with a rapid equilibration as long as approximately the same amount of phosphate is released each time fresh water is introduced. These data do not therefore provide particularly useful information regarding desorption kinetics.

2.4.4 Conclusion of Kinetics Data Analysis

As discussed above, the kinetics model is not very useful for our analysis. However it showed that the time of equilibration in the batch experiments used to calibrate our model (48 hours) was probably too short. Despite this shortcoming, the equilibrium model remains the best and easiest approach to the problem. It is therefore used in the following sections to discuss the behavior of phosphorus in the system.

## 2.5 Analysis of Buffer Capacity and Desorption using the Equilibrium Model

The column experiments shown in Figures 6a and 6b give pH of the effluent water as a function of time. It can be seen that the effluent water is buffered around pH=6.8

when C_3=0.49 mg/L, and around pH=6.3 when C_4=6.1 mg/L, even though the pH of input groundwater was 5.5. In order to understand where this buffering capacity comes from, MINEQL+ can be used to model a process similar to the desorption experiment conducted by the USGS (Walter et al., 1995). The column experiments can be modeled as successive batches of clean groundwater equilibrated with a batch of contaminated sediments. The characteristics of the clean groundwater and the speciation of surface sites initially in equilibrium with contaminated groundwater are calculated using MINEQL+ with the recipe given in the USGS Report. A new recipe using the ionic composition of clean water added to the distribution of contaminated sites is then equilibrated. The process can be repeated as many times as needed, where each pore volume is a new calculation. Table 1 summarizes the inputs in MINEQL+ for the first pore volume.

	Input 1 (M)	Input 2 (M)
TOTH for Clean Groundwater	2.75E-04	2.75E-04
TOTH for Contaminated Groundwater	3.03E-04	2.22E-04
Sum of TOTH	5.78E-04	4.97E-04
TOTC (Clean Groundwater)	1.50E-04	1.50E-04
TOTPO4	1.00E-04	3.15E-05
TOTSites	5.40E-04	5.40E-04

Table 1. MINEQL Input Summary for Iteration 1

The electrostatic double layer modeling in MINEQL+ resulted in a buffering of the water by carbonate which yielded a pH constant around 5.4. The results are shown on Figure 12, for the conditions corresponding to C_3=0.49 mg/l.

31
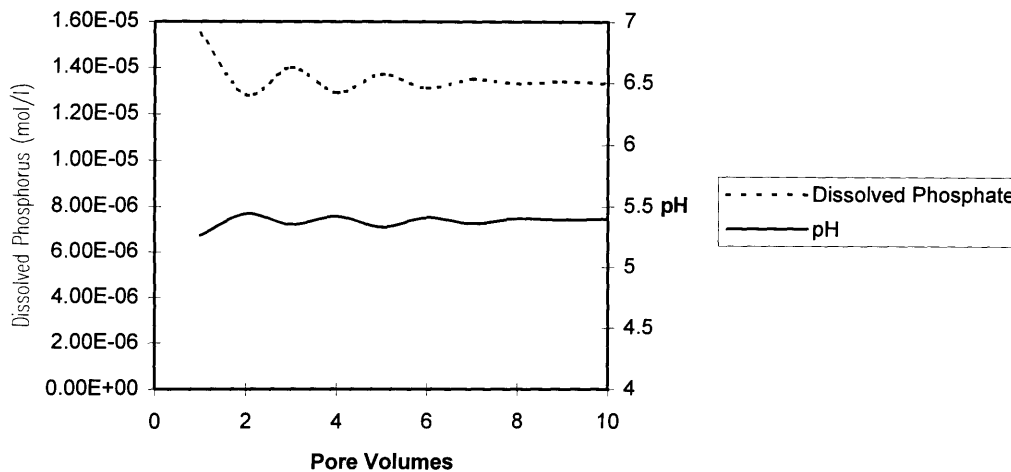
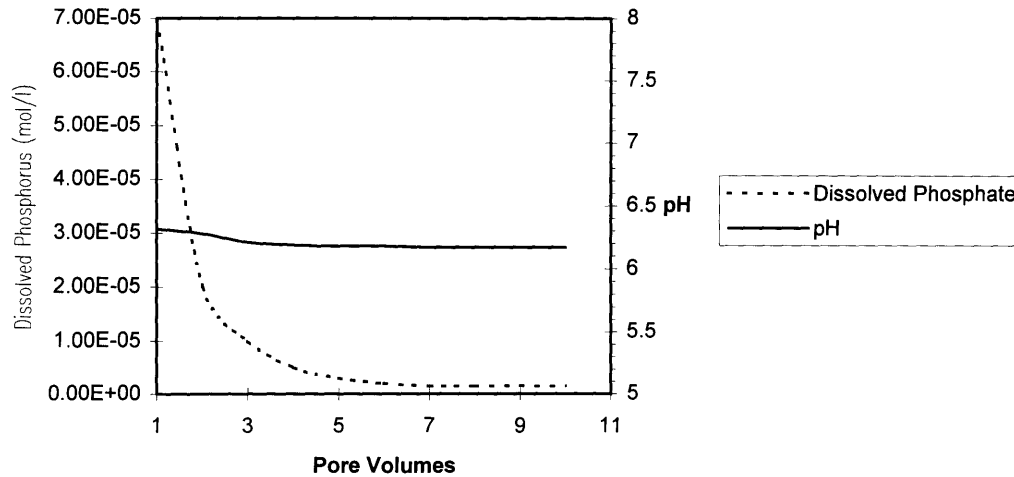**Figure 12. Modeling of Buffering Capacity with Double Layer Model**

The oscillations observed on Figure 12 are probably due to rounding errors in the MINEQL+ results. We see that the phosphate does not get washed away after 10 pore volumes. This is consistent with the number of pore volumes observed on Figure 6a, and we could expect a wash out after 15 to 20 pore volumes.

The pH of the fresh groundwater was originally 5.4 with a buffering by carbonate. We can see that the equilibrium model does not predict the buffering at higher pH observed in the experiment. This result can be explained by the fact that, for average ionic strength values, the double layer model considers the neutral surface site as dominant over a large pH range: since the acid-base speciation of the surface does not change much as a function of pH, little buffering of the solution by the surface can occur. Therefore, the use of this double layer model should not be trusted for pH predictions.

The experiments and the modeling do not give good explanations for the observed buffering. Two species could be responsible for this buffering capacity: the sites themselves and the species $\equiv SPO_4^{3-}$. The sites, namely $\equiv SOH$ and $\equiv SOH_2^+$, could have a traditional buffer effect (the pKa of equation (1) is 6.3). For $\equiv SPO_4^{3-}$, the resulting desorption of PO_4^{3-} (see equation 5) from this contaminated site could also consume an H^+ ion, thus buffering the more acidic fresh groundwater.

32

For comparison, a modeling of the system was done without electrostatic effect, the sites were added to MINEQL+ as complex species (i.e., without any particular surface property). Modeling the sites in this manner results in a pH buffering around pH=6.3. The results of this modeling are shown on Figure 13.

Figure 13. Modeling of Buffering Capacity without Double Layer Model

This type of modeling (without electrostatic effects) appears to be simulating the pH effects relatively accurately. However, the model was not calibrated and does not reproduce the phosphate sorption behavior under any conditions. It could be interesting to calibrate such a model for a further study.

We can also run the same type of calculations to model the desorption of phosphorus observed with the desorption experiment (Figure 4). We assume each addition of fresh water represents a new equilibration, and again neglect any effects of kinetics. The soil was initially equilibrated with a free phosphorus concentration of 3 mg/l. We have the following results (each point of the curves on Figure 4 is the equivalent of one pore volume, since each point corresponds to the introduction of fresh groundwater in the samples) as shown on figure 14.
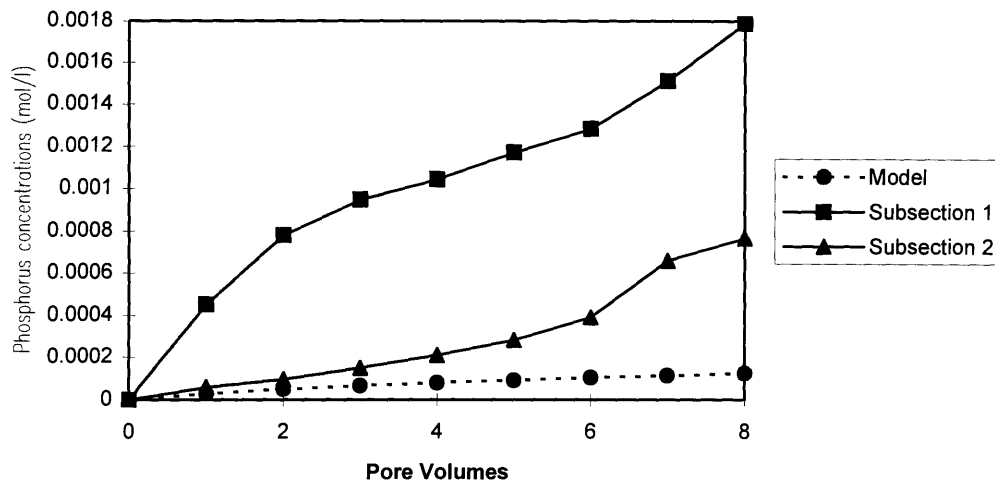
Figure 14. Comparison of Actual and Modeled Desorption Behavior

As seen on the figure above (Figure 14), the modeling of phosphorus sorption with an electrostatic model resulted in values lower than the values given by the experiment. Three possible explanations for this discrepancy are that, 1) the pH effects are either different in the experiment or not well reproduced in the modeling (for example in the previous modeling, the pH is given by the model and differs from the actual pH), or 2) the experiments have non representative time-scales, or 3) higher desorption is due to colloidal mobilization (same effect as in the column experiments).

2.6 Analysis of Discharge Predictions

In 1984, the easternmost four disposal beds were abandoned. In 1993, the USGS study showed that rapid phosphorous desorption, analogous to the concentration peak observed in the column experiment data (See Figures 6a and 6b), was likely to occur in the aquifer (Walter, 1995). The phosphorus peak exhibited by the column experiments cannot be explained by equilibrium behavior. Stollenwerk (1995) proposed that the peak might be associated with pH effects. As clean groundwater is flushed through the sediments, the pH change produces a sudden release of phosphorus.

However, this explanation may not be valid. The first reason is that in the column experiments, the pH peak is either very small (Figure 6a) or it follows the phosphorus peak instead of preceding it (Figure 6b). The second reason is that the modeling with MINEQL+™ as well as the data from the pH isotherms show that a pH change of 0.5 is not enough to produce such a peak (Table 2).

	Initial Concentration (mol/l)	Observed Peak (mol/l)	MINEQL Prediction (mol/l)
Column experiment with C_3=0.49 mg/l Figure 6a	1.23E-05	2.74E-05	1.50E-05
Column experiment with C_4=6.1 mg/l Figure 6b	1.97E-04	2.58E-04	2.10E-05

Table 2. Comparison of observed peak and predicted peaks for a half unit pH upward shift

We see that in the case of the experiment with C_4=6.1 mg/l (Figure 6b), the predicted discharge is close to the observed peak. And in this experiment the recorded pH shows an upward shift of half unit. But in the first column experiment, the peak is clearly not predicted by isotherms or by the modeling.

An alternative explanation for this peak is colloidal mobilization. As the clean groundwater reaches the contaminated sediments, it produces a change that mobilizes colloids. The change that causes this effect can be hypothesized to be the change in ionic strength, which decreases by one order of magnitude in clean groundwater (data from USGS gives an ionic strength of 400 µmol/l for clean groundwater and 3000 µmol/l for contaminated groundwater); as clean groundwater reaches the contaminated zone, the decrease of ionic strength can cause the colloids and the phosphate associated with them to mobilize.

This behavior of phosphorus mobilization may affect greatly the predictions of phosphorus discharge in the pond. The actual discharge predictions are based on

observed phosphorus concentrations in the plume along a flow line. They do not take the peak effect into account. These effects are not very well quantified, but the column experiments show that peak concentrations could be twice the value expected from equilibrium calculations.

The buffer capacity exhibited by the sediments (as discussed in the previous section) will not hinder the high desorption. A higher pH means more desorption, as shown by the pH isotherms.

The predictions could also be underestimating the actual total discharge. The reason for this underestimation could be that the total amount of phosphorus in the contaminated sediments, as determined by core extractions with 1M HCl (Walter, 1995), is far greater than the concentrations of surface sorbed phosphorus (according to the equilibrium model). However, this extractable phosphorus will probably be desorbing or dissolving via a much slower process, and will thus not affect the peak discharge as the rapid desorption of surface-sorbed phosphorus will.

3. CONCLUSION

In the present study, the mechanisms of transport of phosphorus in the STP Plume have been studied. The data was obtained from former studies on the phosphorus plume at MMR by the US Geological Survey (USGS). Two chemical models, an equilibrium model (MINEQL+) and a kinetic model (AcuChem), were applied to the data sets to try to model the sorption behavior of phosphorus in the plume.

It is shown that the equilibrium model provides a reasonable approximation of phosphate sorption behavior on short time scales, although it is unable to predict the observed buffering pH by the sediments. The kinetic model does not provide significant additional information. It is inconclusive regarding the long-term sorption and desorption of phosphate, since it is based on experiments lasting only a few days. Only the equilibrium model was therefore used to model desorption behavior given observed pH changes in the sediments. The modeling results suggest that the discharge predictions made by the USGS may be underestimating the real discharge in the next years. Factors such as pH effects, colloid mobilization and slow desorption of long term sorbed phosphorus may be significant but are still poorly understood.

GLOSSARY

anaerobic- containing no oxygen or nitrate

anoxic - containing no oxygen

batch experiment (batch study) - experiment where the soil sample is mixed with groundwater and left to equilibrate

buffer capacity - capacity of an aqueous solution to remain at a constant pH

calibration - the procedure by which a model is adjusted to be able to fit actual data

carbonate species - one of the following species: CO_3^{2-}, HCO_3^-, H_2CO_3, CO_2

colloid - small metallic particle

colloidal mobilization - physical phenomenon where colloids are suspended in the groundwater

column experiment (column study) - experiment where soil samples are packed into columns and where groundwater in flushed through the columns

downgradient - in the direction of decreasing hydraulic head

electric double layer model - adsorption theory where the sorption sites are represented by two physical layers

eutrophic - a condition of high nutrient content in a surface water body, leading to heavy biological productivity

eutrophication - an increased growth of aquatic biota, particularly algae and macrophytes, relative to the normal rate of productivity in the absence of perturbations to the system

hydraulic head - the level to which water will rise, due to potential and kinetic energy of ground water, in a piezometer that is placed in an aquifer

hydraulic gradient - the change in hydraulic head over distance

infiltration beds - sandy areas where the treated groundwater is discharged and can rapidly infiltrate in the soil

ionic - having a net electrical charge

isotherm - measurement made at constant temperature

isoconcentration contour - A map contour delimiting the boundaries of a single concentration value

nutrient - elements and compounds necessary for biological processes to occur

organic - containing the elements carbon and hydrogen

oxide - pure specie associated with one or several oxygen

oxidized - during reduction/oxidation reactions, the loss of one or more electrons

oxyhydroxide - oxide with water molecules

plume - an area of pollution in any environmental medium

recharge zone - area recharging surface waters

reduced - during reduction/oxidation reactions, the gain of one or more electrons

remediation - clean-up or restoration of contaminated site

retardation - physical phenomenon where the transport of a chemical specie in the soil is retarded

sorption site - chemical specie on which another specie can be fixed

steady state - when conditions are not significantly changing over time

till - densely packed glacial deposits

unsaturated zone (vadose zone) - zone situated above the water table

vertical gradient - a hydraulic gradient in the vertical direction

REFERENCES

Braun, W., Herron, JT., and Kahaner, D.K., 1988. *Acuchem: a computer program for modeling complex chemical reaction systems*, Int. J. Chem. Kinetics, vol. 20, p. 51-62

Dzombak, D.A., Morel, F., 1990. *Surface Complexation Modeling*, Hydrous Ferric Oxide, New York, John Wiley

Goldberg, S., 1984. *A chemical Model of Phosphate Adsorption by Soils*, Soil Sci. Soc. Am. J., vol. 48

Gschwend, P.M., 1987. *Monodisperse Ferrous Phosphate Colloids in an Anoxic Groundwater Plume*, Journal of Contaminant Hydrology, vol. 1, p. 309-327

Isenbeck-Schroter, M., Doring, U., 1993. *Experimental approach and simulation of the retention processes limiting orthophosphate transport in groundwater*, Journal of Contaminant Hydrology, vol. 14, p. 143-161

LeBlanc, D.R., 1984a. Sewage Plume in a Sand and Gravel Aquifer, Cape Cod, Massachusetts. Water Supply Paper 2218. U.S. Geological Survey, Denver, Colorado

LeBlanc, D.R., 1984a. *Movement and Fate of Solutes in a Plume of Sewage-Contaminated Ground Water, Cape Cod, Massachusetts: U.S. Geological Survey Toxic Waste Ground-Water Contamination Program*, Toxic Waste Technical Meeting, Tucson, AZ, March 20-22, 1984, U.S.G.S. Open-File Report 84-475

LeBlanc, D.R., 1984b. *Digital Modeling of Solute Transport in a Plume of Sewage-Contaminated Groundwater*, In: D.R. LeBlanc, editor. Movement and Fate of Solutes in a Plume of Sewage-Contaminated Groundwater, Cape Cod, Massachusetts. U.S. Geological Survey Toxic Waste Groundwater Contamination Program. Papers presented at the Toxic Waste Technical Meeting, Tucson, Arizona, March 20-22, 1984. Open-File Report 84-475. U.S. Geological Survey, Boston, Massachusetts

LeBlanc, D.R., 1984b. *Sewage Plume in a Sand and Gravel Aquifer*, U.S.G.S. Water Supply Paper 2218

Lijklema, L., 1980. *Interaction of Orthophosphate with Iron(III) and Aluminum Hydroxides*, Soil Sci. Soc. Am. J., vol. 14

Mansell, R.S.,1977. *Experimental and Simulated Transport of Phosphorus Through Sandy Soils*, Water Resources Research, vol. 13, p. 189-193.

Morel, F., 1993. Principles and applications of Aquatic Chemistry, New York, John Wiley.

Munns, D. N., 1976. *Kinetics and Equilibrium in Some Tropical Soils*, Soil Sci. Soc. Am. J., vol. 40, p. 46-51

Robertson, W.D., 1995. *Development of steady-state phosphate concentrations in septic system plumes*, Journal of Contaminant Hydrology, vol. 19, p. 289-305

Stollenwerk, K.G., 1995. *Modeling the effects of Variable Groundwater Chemistry on Adsorption of Molybdate*, Water Resources Research, vol. 31, p.347-357

Stollenwerk, K.G., 1996. *Simulation of phosphate transport in sewage-contaminated groundwater, Cape Cod, Massachusetts*, Applied Geochemistry, vol. 11, p.317-324

Van der Zee, S., 1989. *Prediction of Phosphate Transport in Small Columns With an Approximate Sorption Kinetics Model*, Water Resources Research, vol. 25, p. 1353-1365

Van Riemsdijk, W.H., 1984. *Phosphate Sorption by Soils*, Soil Sci. Soc. Am. J., vol. 48

Walter, D.A., B.A. Rea, K.G. Stollenwerk, and J. Savoie, 1995. Geochemical and Hydrologic Controls on Phosphorus Transport in a Sewage-Contaminated Sand and Gravel Aquifer Near Ashumet Pond, Cape Cod, Massachusetts. Water-Resources Investigations Report 95-381. U.S. Geological Survey, Marlborough, Massachusetts

Walter, D.A., Bussey, K.W., 1996. Spatial and Temporal Distribution of Specific Conductance, Boron, and Phosphorous in a Sewage-Contaminated Aquifer Near Ashumet Pond, Cape Cod, Massachusetts, U.S. Geological Survey, Open-File Report 96-472

Westall, J.C., 1976. Mineql: a computer program for the calculation of chemical equilibrium composition of aqueous systems, Massachusetts Institute of Technology, Ralph M. Parsons Laboratory for Water Resources and Hydrodynamics, Technical Note N.18